



NRC Publications Archive Archives des publications du CNRC

The IGF-trap: novel inhibitor of carcinoma growth and metastasis

Wang, Ni; Rayes, Roni F.; Elahi, Seyyed Mehdy; Lu, Yifan; Hancock, Mark A.; Massie, Bernard; Rowe, Gerald E.; Aomari, Hafida; Hossain, Sazzad; Durocher, Yves; Pinard, Maxime; Tabaries, Sébastien; Siegel, Peter M.; Brodt, Pnina

This publication could be one of several versions: author's original, accepted manuscript or the publisher's version. / La version de cette publication peut être l'une des suivantes : la version prépublication de l'auteur, la version acceptée du manuscrit ou la version de l'éditeur.

For the publisher's version, please access the DOI link below. / Pour consulter la version de l'éditeur, utilisez le lien DOI ci-dessous.

Publisher's version / Version de l'éditeur:

<https://doi.org/10.1158/1535-7163.MCT-14-0751>

Molecular Cancer Therapeutics, 14, 4, pp. 982-993, 2015-02-11

NRC Publications Record / Notice d'Archives des publications de CNRC:

<https://nrc-publications.canada.ca/eng/view/object/?id=82c3e9ff-bb92-4e4b-a320-669e049fe750>

<https://publications-cnrc.canada.ca/fra/voir/objet/?id=82c3e9ff-bb92-4e4b-a320-669e049fe750>

Access and use of this website and the material on it are subject to the Terms and Conditions set forth at

<https://nrc-publications.canada.ca/eng/copyright>

READ THESE TERMS AND CONDITIONS CAREFULLY BEFORE USING THIS WEBSITE.

L'accès à ce site Web et l'utilisation de son contenu sont assujettis aux conditions présentées dans le site

<https://publications-cnrc.canada.ca/fra/droits>

LISEZ CES CONDITIONS ATTENTIVEMENT AVANT D'UTILISER CE SITE WEB.

Questions? Contact the NRC Publications Archive team at

PublicationsArchive-ArchivesPublications@nrc-cnrc.gc.ca. If you wish to email the authors directly, please see the first page of the publication for their contact information.

Vous avez des questions? Nous pouvons vous aider. Pour communiquer directement avec un auteur, consultez la première page de la revue dans laquelle son article a été publié afin de trouver ses coordonnées. Si vous n'arrivez pas à les repérer, communiquez avec nous à PublicationsArchive-ArchivesPublications@nrc-cnrc.gc.ca.



The IGF-Trap: Novel Inhibitor of Carcinoma Growth and Metastasis

Ni Wang¹, Roni F. Rayes¹, Seyyed Mehdy Elahi², Yifan Lu¹, Mark A. Hancock³, Bernard Massie^{2,4}, Gerald E. Rowe², Hafida Aomari², Sazzad Hossain², Yves Durocher², Maxime Pinard¹, Sébastien Tabariès^{5,6}, Peter M. Siegel^{5,6,7}, and Pnina Brodt^{1,5,8}

Abstract

The IGF1 receptor promotes malignant progression and has been recognized as a target for cancer therapy. Clinical trials with anti-IGF1R antibodies provided evidence of therapeutic efficacy but exposed limitations due in part to effects on, and the compensatory function of, the insulin receptor system. Here, we report on the production, characterization, and biologic activity of a novel, IGF-targeting protein (the IGF-Trap) comprising a soluble form of hIGF1R and the Fc portion of hIgG₁. The IGF-Trap has a high affinity for hIGF1 and hIGF2 but low affinity for insulin, as revealed by surface plasmon resonance. It efficiently blocked IGF1R signaling in several carcinoma cell types and inhibited tumor cell proliferation, migration, and invasion *in vitro*. *In vivo*, the IGF-Trap showed favorable phar-

macokinetic properties and could suppress the growth of established breast carcinoma tumors when administered therapeutically into tumor-bearing mice, improving disease-free survival. Moreover, IGF-Trap treatment markedly reduced experimental liver metastasis of colon and lung carcinoma cells, increasing tumor cell apoptosis and reducing angiogenesis. Finally, when compared with an anti-IGF1R antibody or IGF-binding protein-1 that were used at similar or higher concentrations, the IGF-Trap showed superior therapeutic efficacy to both inhibitors. Taken together, we have developed a targeted therapeutic molecule with highly potent anticancer effects that could address limitations of current IGF1R-targeting agents. *Mol Cancer Ther*; 14(4); 982–93. ©2015 AACR.

Introduction

The receptor for type I insulin-like growth factor (IGF1R) and its ligands IGF1 and IGF2 play an important role in cancer progression and metastasis (reviewed in refs. 1, 2). Recent evidence has linked the IGF axis to all the major steps in the initiation and progression of malignant disease, including the development and maintenance of the cancer stem cell, epithelial–mesenchymal transition, and regulation of the tumor microenvironment (reviewed in ref. 3).

¹Department of Surgery, McGill University Health Centre, McGill University, Montreal, Québec, Canada. ²Biotechnology Research Institute (National Research Council), Université de Montréal, Montreal, Québec, Canada. ³SPR-MS Facility, McGill University, Montreal, Québec, Canada. ⁴Department of Microbiology and Immunology, Université de Montréal, Montreal, Québec, Canada. ⁵Department of Medicine, McGill University Health Centre, McGill University, Montreal, Québec, Canada. ⁶Rosalind and Morris Goodman Cancer Research Centre, McGill University, Montreal, Québec, Canada. ⁷Department of Anatomy & Cell Biology, McGill University Health Centre, McGill University, Montreal, Québec, Canada. ⁸Department of Oncology, McGill University Health Centre, McGill University, Montreal, Québec, Canada.

Note: Supplementary data for this article are available at Molecular Cancer Therapeutics Online (<http://mct.aacrjournals.org/>).

N. Wang and R.F. Rayes contributed equally to this article and share first authorship.

Corresponding Author: Pnina Brodt, Research Institute - McGill University Health Center, 1001 Boul Décarie, Site Glen Pavilion E, Room E2-6220 (mail drop point E2-6217), Montréal, QC H4A 3J1, Canada. Phone: 514-934-1934, ext. 36692; Fax: 514-934-4460; E-mail: pnina.brodt@mcgill.ca

doi: 10.1158/1535-7163.MCT-14-0751

©2015 American Association for Cancer Research.

Several inhibitors of the IGF axis have been tested clinically. For example, humanized or fully human neutralizing antibodies against IGF1R are presently being evaluated as monotherapies or in combination with other drugs, for the treatment of various malignancies (4, 5). In addition, neutralizing antibodies [MEDI-573 (6), BI836845 (7)] and recombinant IGF-binding proteins (IGFBP; refs. 8, 9) that react with IGF1 and IGF2 and small-molecule tyrosine kinase inhibitors have also been developed and some have advanced into clinical trials (reviewed in refs. 3, 10, 11). The results of early and more advanced clinical trials with some of these inhibitors exposed several obstacles to their successful use in cancer therapy (12). Because of the homology between IGF1R and the insulin receptor (IR), several inhibitors of IGF1R signaling (including tyrosine kinase inhibitors) were found to also disrupt IR signaling, resulting in undesirable side effects such as hyperinsulinemia and hyperglycemia. The responses to more specific drugs, such as anti-IGF1R antibodies, were also disappointing, and this has been attributed to several potential factors, including (i) a compensatory feedback mechanism that leads to increased IGF production due to increased growth hormone release (13) and (ii) insulin receptor isoform A (IR-A) signaling that can be initiated by IGF2 (the main plasma IGF1R ligand in humans) or insulin and lead to enhanced tumor cell growth (14–16). New insight into IGF1R signaling regulation has also recently led to the proposition that the targeting of IGF1R by antibodies or kinase inhibitors may result in alternative, kinase-independent, ERK signaling mediated via recruitment of interacting proteins such as β arrestins, thereby limiting the effectiveness of these inhibitors (17). Some anti-IGF1R antibodies have been withdrawn from clinical trials due to lack of benefit

(CP-751871, Pfizer; RG1507, Roche; ref. 10), whereas others are currently being tested in combination with other drugs.

An effective strategy for blocking the action of cell surface receptors is the use of soluble decoys that bind the ligand with high affinity and reduce its bioavailability to the cognate receptor in a highly specific manner (18–20). For example, a soluble TNF α receptor–Fc fusion protein (Etanercept or Enbrel) is currently in clinical use for the treatment of rheumatoid arthritis (21) and a VEGFR1/VEGFR2-Fc decoy (VEGF Trap) is in clinical trials as an antiangiogenic, anticancer drug (18). Although the development of IGFIR decoys for cancer treatment has been reported (22), to date, none have advanced into clinical use.

A soluble IGFIR receptor decoy offers key advantages over receptor targeting antibodies and small-molecule inhibitors. With high specificity for IGF1 and IGFII, and an expected poor affinity for insulin, a decoy should have minimal negative effects on the IR system. Because the decoy binds circulating ligands, penetration and diffusion into tumor sites are not major obstacles. Moreover, although antibodies to IGFIR or receptor-specific inhibitors do not target IR-A/IGFII-initiated signaling, a decoy receptor with high binding affinities for both circulating ligands should reduce IGFII bioavailability and IR-A activation.

Previously, we reported that metastatic lung carcinoma cells genetically engineered to produce a 933-amino acid, soluble protein spanning the entire extracellular domain of the IGFIR (sIGFIR), failed to produce liver metastases in 88% of injected mice, resulting in increased long-term, disease-free survival (23). Subsequently, we developed a novel therapeutic approach for sustained *in vivo* delivery of this soluble receptor by genetically engineered autologous bone marrow stromal cells (24), and this resulted in growth inhibition of several tumor types, due to reduced tumor cell growth and increased apoptosis. More recently, a third-generation gutless adenovirus engineered to express the soluble receptor was used for sustained production of the soluble receptor *in vivo*, and this resulted in protection of the animals from tumor growth in the liver (25).

Here, we describe the production, characterization, pharmacokinetic properties, and therapeutic potency of the next-generation decoy—a recombinant soluble protein consisting of the extracellular domain of human IGFIR fused to the Fc portion of human IgG₁ (the IGF-Trap). We show that this novel IGF-Trap was highly effective *in vivo* in multiple preclinical models of aggressive carcinoma types, causing regression of established tumors and comparing favorably with an anti-hIGFIR antibody and an IGF-binding protein. Collectively, these data identify the IGF-Trap as a potential anticancer drug.

Materials and Methods

Cells

The origins and metastatic properties of murine colon carcinoma MC-38 and Lewis lung carcinoma subline H-59 cells and their culture conditions and testing were described in detail elsewhere (24). MC-38 cells were originally from an NCI repository and were obtained as a kind gift from Dr. Shoshana Yakar (New York University, NY) in 2005. They were recently authenticated by Didion and colleagues (26) using SNP profiling as described. H-59 is a subline of the Lewis lung carcinoma that was developed by the Brodt laboratory in 1986, as previously described in detail (27). The 4T1 and MDA-MB-231 cell lines were obtained from the ATCC in 2002. Subline 2776 of 4T1 was

obtained in 2010, as previously described (28). All cell lines were periodically tested for mouse and human pathogens and mycoplasma infection, as per the McGill University Animal Care committee and the McGill University Biohazard committee guidelines, and were last retested in 2014. To avoid cross-contamination and phenotype changes, these cell lines have not been maintained in long-term cultures. All cells used in this study were maintained as frozen stocks and cultured for 2 to 4 weeks only in DMEM (MC-38, MDA-MB-231) or RPMI (H-59, 4T1) media supplemented with 10% FBS and antibiotics before use in the experiments. Authentication of these cell lines based on morphology, growth curve analysis, and metastatic phenotype was performed regularly, and no phenotype changes were observed through the duration of this study.

Reagents and antibodies

Recombinant mIGFI was from Cedarlane and R&D Systems, rhIGFI was from Cedarlane and BioVision, rhIGFII was from Calbiochem (EMD-Millipore/ThermoFisher) and BioVision, and human insulin was from Sigma-Aldrich. The mouse monoclonal antibody to human IGFIR-MAb 391 (R&D Systems; ref. 29) was used to treat tumor-bearing mice *in vivo*. For IHC, rabbit polyclonal antibodies to pIGFIR, Ki67, and cleaved caspase-3 (all from Abcam) and a rat monoclonal antibody to CD31 (Clone MEC 13.3) from BD Biosciences were used. Secondary antibodies Alexa Fluor 647-goat-anti-rabbit and Alexa Fluor 568-goat anti-rat antibodies from Molecular Probes were used as appropriate.

Generation of CHO cells stably producing IGF-Traps

The construction of the sIGFIR and IGF-Trap is detailed in Supplementary Materials and Methods. Lentivirus particles expressing sIGFIR or IGF-Trap were generated in the packaging cell line 293PaLV, as detailed previously (30). Two stable cell lines (CHO-cum2-CR5-sIGFIR and CHO-cum2-CR5-IGF-TRAP) were generated by transduction of the CHO-Cum2 cell line with the respective lentivirus particles using the protocol described previously (31). Clonal populations of the transduced cells were obtained by limiting dilution and clones identified as highest producers were expanded. Protein production was initiated by the addition of 1 μ g/mL cumate in fresh medium, followed by 24-hour incubation at 37°C, and 7 to 8 days incubation at 30°C. Cells were removed by centrifugation, and the supernatants were filtered and concentrated (10 \times) using the Tangential Flow Filtration Systems (Pellicon ultrafiltration cassettes; EMD-Millipore). The sIGFIR and IGF-Trap fusion proteins were purified on ceramic hydroxyapatite (type I) columns (CHT; Bio-Rad) followed by size exclusion chromatography performed on Sephacryl S400 HR columns (GE Healthcare), and the purity of the eluted proteins was verified by SDS-PAGE. Where indicated, further purification using protein A columns was performed using a MabSelect SuRe column (8 ml; GE Healthcare). The proteins were stored at –80°C until used for the analyses described.

Production of the rhIGFBP-1

The construction of rhIGFBP-1 is described in Supplementary Materials and Methods. The IGFBP-1 was purified by sequential affinity chromatography on Fractogel EMD-chelate (EMD-Millipore) charged with cobalt. The purified protein was desalted in PBS on a desalting column (GE Healthcare) as per the manufacturer's instruction.

Surface plasmon resonance

Binding of mIGFI, hIGFI, hIGFII, and human insulin to sIGFIR, IGF-Trap, or IGFBP-1 was examined using label-free, real-time BIACORE 3000 instrumentation (GE Healthcare). Experiments were performed on research-grade CM5 sensor chips. Purified sIGFIR and IGF-Trap preparations (15 $\mu\text{g}/\text{mL}$ in 10 mmol/L sodium acetate, pH 4.5) were immobilized using the Biacore Amine Coupling Kit [4,000–8,000 resonance units (RU) final]; corresponding reference surfaces were prepared in the absence of any IGF-Trap. Maltose-binding protein (negative control) and ligands were injected over reference and receptor-immobilized surfaces in-tandem, using variable flow rates (10, 25, 50 $\mu\text{L}/\text{min}$) and contact times (5–20 minutes association/dissociation), and sensor chip surfaces regenerated between sample injections. Between sample injections, surfaces were regenerated at 50 $\mu\text{L}/\text{min}$ using two 30-second pulses of solution A (1 mol/L imidazole) and B [0.03% (v/v) Empigen detergent in 1/10 diluted Pierce Gentle Elution buffer]. SPR data were double-referenced (32) and are representative of duplicate injections acquired from at least two independent trials. The binding of hIGFI and -II to amine-coupled IGFBP-1 (10 $\mu\text{g}/\text{mL}$ in 10 mmol/L NaOAc, pH 4.5; 600–800 RU final) was examined in a similar manner. Consistent with previous IGF-based SPR methods (33–36), individual association (k_a) and dissociation (k_d) rate constants, as well as overall equilibrium dissociation constants (K_D), for the IGF titrations were determined by global fitting of the data to a "1:1 kinetic" model (BIAevaluation v4.1 software; GE Healthcare). K_D values for the insulin titrations were determined by global fitting of the data to a "steady-state affinity" model in BIAevaluation.

Functional *in vitro* assays

Tumor cell proliferation was measured using the colorimetric MTT assay, as described (23).

Anchorage-independent cell growth was measured using the semi-solid agar clonogenicity assay, as described (37). IGF1 with or without the IGF-Trap was added to the agar overlay and replenished 2 to 3 times weekly for 14 days. Colonies with a diameter of $\geq 80 \mu\text{m}$ were scored.

Apoptosis was analyzed using the anoikis assay, as described previously (38), and the *In Vivo* Cell Death Detection-RED staining Kit (Roche Diagnostics) for quantification.

Cell migration was analyzed using a standard Boyden Chamber assay (37) or a real-time, electrical-impedance-based technique with the automated xCELLigence system (Roche Diagnostics; ref. 39). Tumor cells were plated in wells (5×10^4 cells/well) of CIM-Plates 16 (Roche Diagnostics) and placed on top of a lower chamber containing 10^4 ng/dL IGFII in SF media with or without the IGF-Trap. Incubation at 37°C was for 12 hours with continuous reading and recording by the xCELLigence software.

Cell invasion was also measured with the xCELLigence system. Tumor cells were plated at 5×10^4 cells per well in CIM-Plates 16 on membranes precoated with a 1:40 dilution of Matrigel (BD Biosciences), placed on top of a lower chamber containing 5,000 ng/dL IGF1 with or without the IGF-Trap at the indicated molar ratios and incubated at 37°C for 48 hours.

Pharmacokinetic analysis

Mice were injected intravenously with 10 mg/kg IGF-Trap. The mice were divided into several groups of 3 mice each and blood collected from alternate groups, beginning at 5 minutes and up to 10 days after injection. Plasma IGF-Trap levels were analyzed

using the soluble IGFIR ELISA Kit (R&D Systems). Data for each group of mice bled at the same interval were pooled. Noncompartmental analysis was performed using Phoenix Win-Nonlin Software v6.2 (Pharsight Corporation), and pharmacokinetic parameters were determined.

Measurement of pAKT

To measure the effect of the IGF-Trap on ligand-induced IGFIR signaling, tumor cells cultured overnight in serum-free media were stimulated for 2 or 20 minutes (as determined based on preliminary experiments) with 10^4 ng/dL IGF1 in the presence or absence of the IGF-Trap that was added at a molar ratio of 2:1. The cells were lysed (40) and pAKT levels in the cell lysates quantified using the RayBio Phospho Akt (Ser473) ELISA Kit (PEL-Akt-S473-T; Raybiotech) as per the manufacturer's instructions.

Measurement of plasma IGF1 and insulin levels

IGF1 was quantified using the mouse IGF-I DuoSet ELISA Kit (R&D Systems), circulating Trap:IGF1 complexes were semiquantified using a combination ELISA, as we previously described (24), and insulin was quantified using the Mercodia mouse insulin ELISA Kit (Mercodia AB). Plasma obtained from mice injected with vehicle only (PBS) was used to establish baselines.

Orthotopic breast cancer models

All mouse experiments were carried out in strict accordance with the recommendations of the Canadian Council on Animal Care (CCAC) and under the conditions and procedures approved by the Animal Care Committee of McGill University (AUP number: 5733). Mammary carcinoma 4T1 cells were injected into the mammary fatpads (MFP) of Balb/c female mice (Charles River) using 5×10^4 cells in 0.05 mL PBS. Tumors were measured on alternate days using a caliper, and tumor volumes were calculated using the formula $1/2 (\text{length} \times \text{width}^2)$. One million MD-MBA-231 cells in 0.05 mL Matrigel diluted 1:1 with PBS were implanted in the MFPs of Ncr nu/nu mice (Taconic Farm). When tumors were established ($50\text{--}100 \text{mm}^3$), the animals were randomized and treated with the indicated concentrations of IGF-Trap, MAb 391, or vehicle (i.v.), twice weekly until day 33. Longitudinal bioluminescence imaging was performed following the i.p. injection of 150 mg/kg XenoLight Rediject D-Luciferin using the IVIS Spectrum/200 (Caliper Lifesciences; Caliper/PerkinElmer).

Experimental metastasis assays

Experimental liver metastases were generated by intrasplenic/portal injections of 5×10^4 (MC-38) or 10^5 (H-59) tumor cells into C56BL/6 mice (Charles River) followed by splenectomy, as previously described (23, 37). Treatments with the IGF-Trap or IGFBP-1 were as indicated. Metastases were scored as previously described (23).

IHC and confocal microscopy

IHC and confocal microscopy were performed as previously described (40) using the indicated antibodies. The sections were analyzed with a Zeiss LSM 780 laser scanning confocal microscope (Carl Zeiss Canada Ltd) equipped with a Zen image analysis station.

Statistical analysis

All cell-based data (*in vitro* assays and IHC) and tumor volumes were analyzed by the two-tailed Student *t* test. The nonparametric Mann-Whitney test was used to analyze experimental metastasis

data, and the Mantel-Cox and Gehan–Breslow–Wilcoxon tests were used to analyze survival data.

Results

Production of an IGF-Trap with high binding affinity and specificity

The engineering and production of the IGF-Trap involved two steps. Initially, we generated a soluble receptor decoy (sIGFIR) consisting of the entire extracellular domain of the receptor (933 amino acid residues = ~370 kDa; Supplementary Fig. S1A) and confirmed its high binding affinity for hIGFI and its specificity, using SPR (Supplementary Fig. S1B and S1C; Supplementary Table S2). To evaluate the biologic activity of this protein, we analyzed its effect on tumor cell proliferation (Supplementary Fig. S2A), invasion (Supplementary Fig. S2B), colony formation in semi-solid agar (Supplementary Fig. S2C), and detachment-induced apoptosis (anoikis; Supplementary Fig. S2D), using the Lewis lung carcinoma subline H-59 cells that are highly responsive to IGF1 (41, 42). These analyses confirmed the IGF1-inhibitory activity of the decoy.

To improve the pharmacokinetic properties of sIGFIR, we generated a sIGFIR–hFc–IgG₁ fusion protein (the IGF-Trap = ~430 kDa) that was produced in CHO cells (Supplementary Fig. S3A). Comparison of the SPR profiles of the native Fc-free sIGFIR (Supplementary Fig. S1B and S1C) and the IGF-Trap (Supplementary Fig. S3B–S3D) revealed that the addition of the Fc

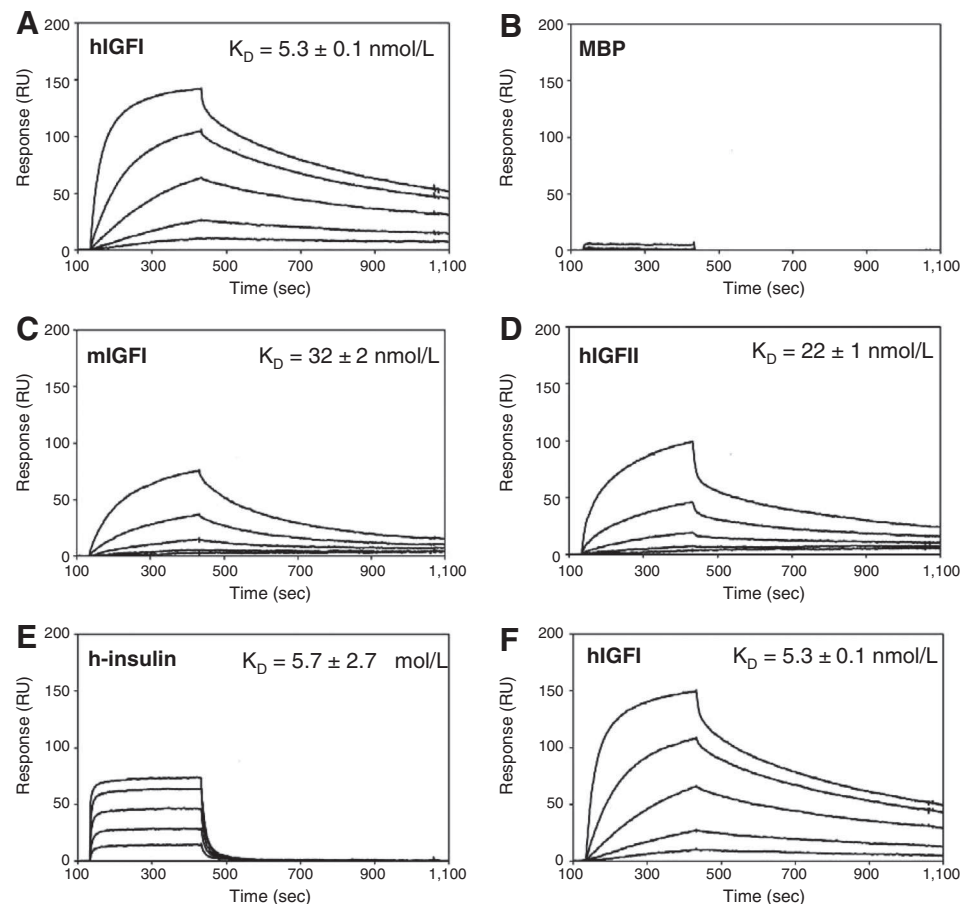
fragment did not alter the individual binding kinetics or overall affinity. Specific dose-dependent binding with the IGF-Trap was most significant with hIGFI (slow-on, slow-off kinetics; Fig. 1A), whereas maltose-binding protein (MBP, negative control; Fig. 1B) exhibited little or no specific binding. Similar slow-on, slow-off kinetics with mIGFI (Fig. 1C) and hIGFII (Fig. 1D) yielded lower binding overall, whereas insulin exhibited distinctly different rapid-on, rapid-off kinetics (Fig. 1E). The observed binding responses correlated well with theoretical R_{max} predictions, and replicate titration series (e.g., for hIGFI; Fig. 1F) generated nearly superimposable data, validating the robustness of the SPR assay. Overall, binding of hIGFI to the IGF-Trap was strongest (K_D ~5 nmol/L; Fig. 1A and Supplementary Table S2) and most stable (i.e., slowest dissociation rate constants), whereas moderately weaker affinities were observed for hIGFI (~22 nmol/L), mIGFI (~32 nmol/L), and a 1,000-fold weaker affinity for insulin (>5 μ mol/L; Fig. 1A; Supplementary Table S2). Taken together, the results confirmed the high affinity and specificity of the IGF-Trap for both hIGFI and hIGFII ligands with K_D values consistent with published data on the native cell surface receptor (34, 36, 43).

The IGF-Trap inhibits IGFIR signaling and blocks IGF1- and IGFII-mediated cellular functions

We next assessed the biologic activity of the IGF-Trap using a series of *in vitro* functional assays with several highly aggressive carcinoma cell types (44, 45). The PI3-K/Akt pathway is

Figure 1.

Binding kinetics and specificity of the IGF-Trap. Shown are representative SPR data for the indicated ligands (3-fold serial dilutions) to amine-coupled IGF-Trap (~8,000 RU) at 25 μ L/min (5-minute association + 10-minute dissociation) at the following concentrations: A, 0–90 nmol/L hIGFI; B, 0–270 nmol/L MBP; C, 0–90 nmol/L mIGFI; D, 0–90 nmol/L hIGFII; E, 0–70 μ mol/L h-insulin; F, to verify the robustness, reliability, and reproducibility of the SPR technique used, a second (repeat) titration of hIGFI was performed following the ordered series shown in A to E. The experimental data were analyzed using the "1:1 kinetic" (hIGFI, hIGFII, mIGFI) or "steady-state affinity" (h-insulin) models in BIAevaluation. The values shown (\pm SE) represent the means of duplicate injections acquired from three independent trials. Theoretical binding maxima were predicted using the equation $R_{max} = (MW_A/MW_L) (R_L/n)$ (n); where R_{max} is maximal binding response (RU) at saturating ligand concentration; MW_A , molecular weight of solution-phase ligand; MW_L , molecular weight of immobilized IGF-Trap; R_L , amount (RU) of IGF-Trap immobilized; n, predicted binding stoichiometry (1:1).



activated downstream of IGFIR phosphorylation and mediates tumor cell rescue from apoptosis (46). In response to IGFI, a marked increase in Akt phosphorylation, as measured by ELISA, was observed in all carcinoma cells tested, and this increase was abolished in the presence of the IGF-Trap (Fig. 2A). This blockade of IGFIR signaling was also reflected in a loss of IGFIR-mediated cellular activities, such as proliferation (Supplementary Fig. S4A), anchorage-independent growth (Supplementary Fig. S4B), invasion (Fig. 2B), and rescue from detachment-induced apoptosis (Fig. 2C) in the presence of IGFI, as measured using lung carcinoma H-59 cells. Similarly, cell migration in response to IGFI or IGFI, as measured using mammary carcinoma 4T1 (Fig. 2D and Supplementary Fig. S4C) or colon carcinoma MC-38 (Fig. 2E) cells, was blocked in the presence of the IGF-Trap. For each cell type, assays and conditions were selected based on preliminary optimization studies. Collectively, these results showed that the IGF-Trap was

biologically active, able to block IGFIR signaling and functions in different cell types, suppress a range of cellular activities essential for cancer growth and metastasis, and inhibit the response to both IGFI and IGFI.

Improved pharmacokinetic properties of the IGF-Trap

To compare the pharmacokinetic properties of sIGFIR and the IGF-Trap *in vivo*, mice received a single 10 mg/kg i.v. injection of the proteins and underwent a serial blood collection for up to 240 hours thereafter. Plasma concentrations were evaluated by ELISA. The area under the plasma drug concentration–time curve (AUC), which reflects the actual body exposure to the drug after administration (Fig. 3A and B; Supplementary Table S3), was increased 4-fold (from 98 to 405 $\mu\text{g} \cdot \text{h/L}$) for sIGFIR-Fc as compared with sIGFIR, where the maximum concentration (C_{max}) increased 2-fold (from 28.6 to 55.4), and the plasma half-life increased 2.15-fold (from 21.9 to 47.5 hours). The results indicated that the IGF-

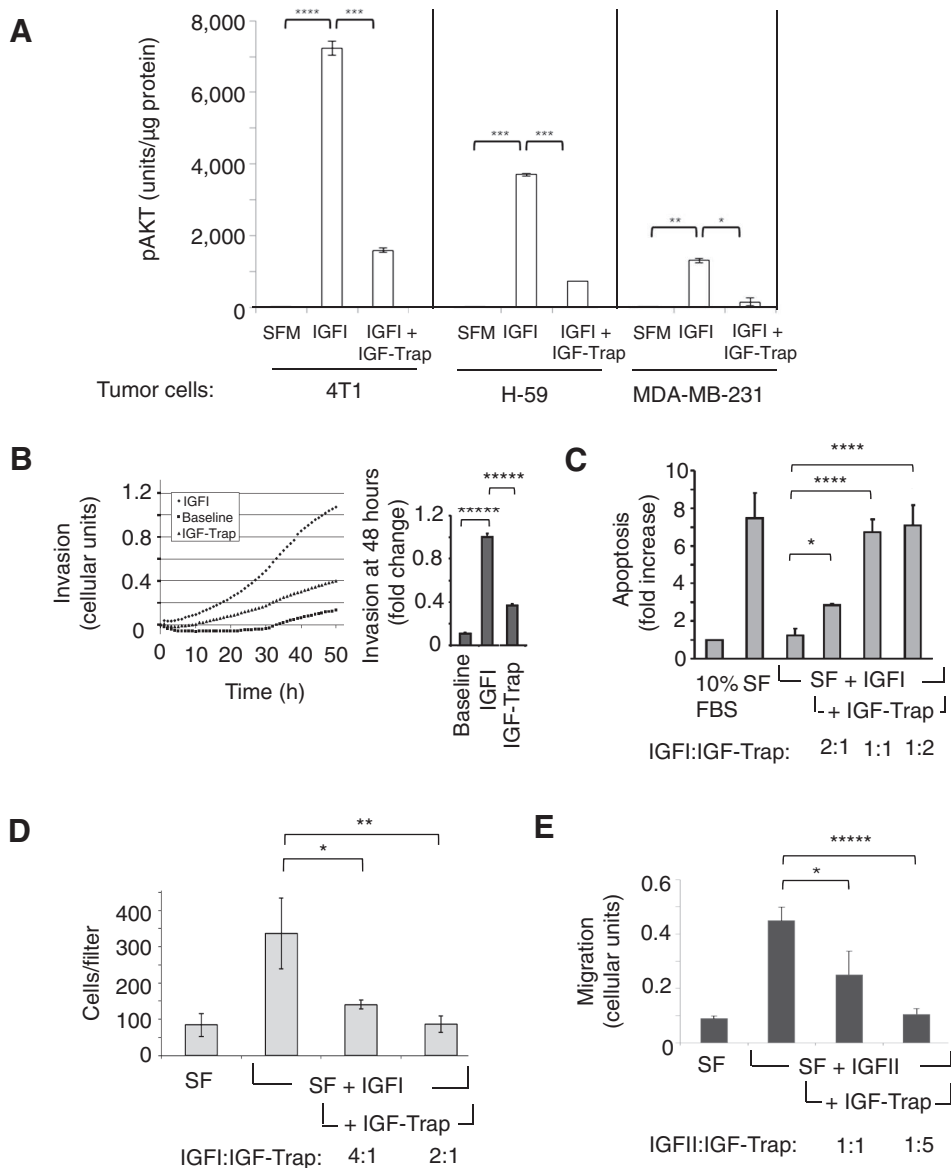


Figure 2.

The IGF-Trap inhibits IGFIR signaling and blocks IGFI- and IGFI-induced cellular activities *in vitro*. Shown are pAKT levels (A) measured following stimulation of the indicated tumor cells for 2 (4T1) or 20 (H-59, MDA-MB-231) minutes with 10^4 ng/dL IGFI, in the presence or absence of the IGF-Trap added at a 2:1 molar ratio (to IGFI). The results are expressed as mean (\pm SE) of triplicate samples. H-59 invasion (B) was measured using the xCELLigence system with 5,000 ng/dL IGFI and the IGF-Trap at a 1:1 molar ratio. Shown are representative results of 5 experiments, each performed in duplicate. Real-time invasion values are shown on the left and relative invasion values at 48 hours on the right. Apoptosis (C) was measured using H-59 cells plated in PolyHEMA-coated wells and incubated for 48 hours with 1,000 ng/dL IGFI with or without the IGF-Trap at the indicated molar ratios. Shown are representative results of 3 experiments expressed as a ratio to cells cultured in 10% FBS (\pm SD). Migration of 4T1 cells (D) was measured using a Boyden chamber with 2×10^4 ng/dL IGFI and the IGF-Trap at the indicated molar ratios. The results are mean (\pm SD) of two experiments performed in triplicate. Migration of MC-38 cells (E) in response to 10^4 ng/dL IGFI was measured using the xCELLigence system. Shown are representative results (\pm SEM) of one of 2 experiments, each performed in triplicate. SFM, serum free medium. *, $P < 0.05$; **, $P < 0.01$; ***, $P < 0.005$; ****, $P < 0.001$; *****, $P < 0.0005$.

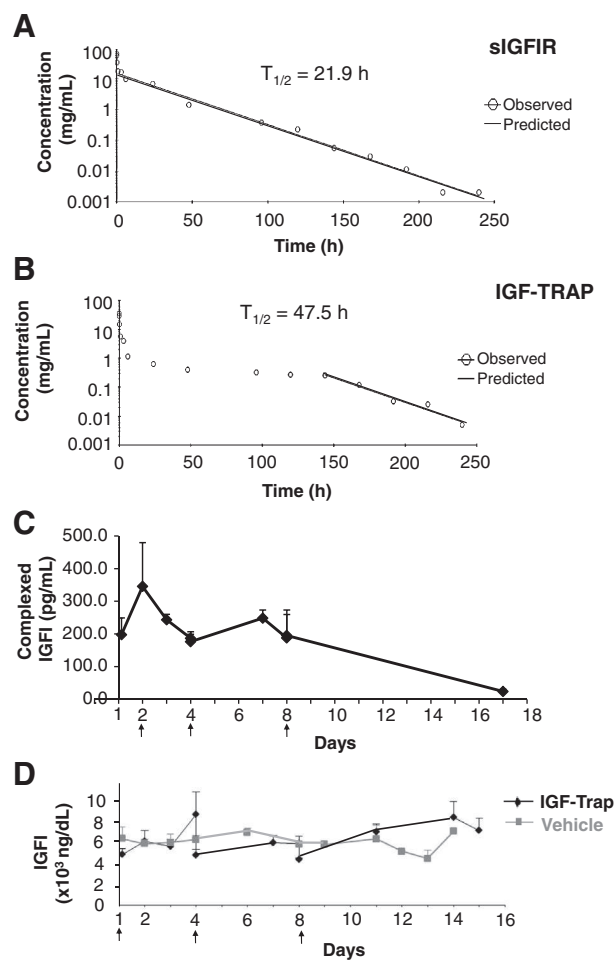


Figure 3. Pharmacokinetic properties and the effect of the sIGFIR and the IGF-Trap on circulating IGFI. Mice were injected intravenously with 10 mg/kg of the purified and LPS-free sIGFIR (A) or 10 mg/kg (A–C) or 5 mg/kg (D) of the IGF-Trap. Soluble IGFIR levels (A and B), IGF-Trap complexes (C), and plasma IGFI (D) were analyzed by ELISA. The results are based on 3 plasma samples per time point. Shown in A and B are results based on 3 serum samples per time point that were analyzed using the PK software (see additional data in Supplementary Table S3). Results in C are mean (\pm SE) of three measurements per time point and represent net values after deduction of background levels that were detected in vehicle-treated mice (35–57 pg/mL). Results in D are expressed as mean (\pm SE) of 3 plasma samples per time point. On days 4 and 8, blood was collected and plasma IGFI concentrations (D) were measured 20 minutes before and 1 hour after IGF-Trap injection.

Trap had significantly improved pharmacokinetics properties in comparison with the native sIGFIR. They also placed the pharmacokinetic properties of the IGF-Trap within the range of other targeted drugs currently in the clinic (18, 47).

We confirmed that in mice injected with the IGF-Trap, sIGFIR:IGFI complexes were detectable within 3 hours of the injection and remained at measurable levels when additional injections were administered every 3 to 4 days, declining progressively after treatment was terminated (Fig. 3C), likely due to proteolytic degradation (48). Total (bound and unbound) circulating IGFI levels during the same period were not significantly different from those in control (vehicle-injected) mice at any of the time points analyzed, although minor fluctuations (up to 15% change) were

observed on the days of IGF-Trap injections (Fig. 3D). Importantly, circulating insulin levels during the same period were not significantly different from those in vehicle-injected mice (Supplementary Fig. S5).

The IGF-Trap inhibits growth of established breast carcinoma tumors and improves survival

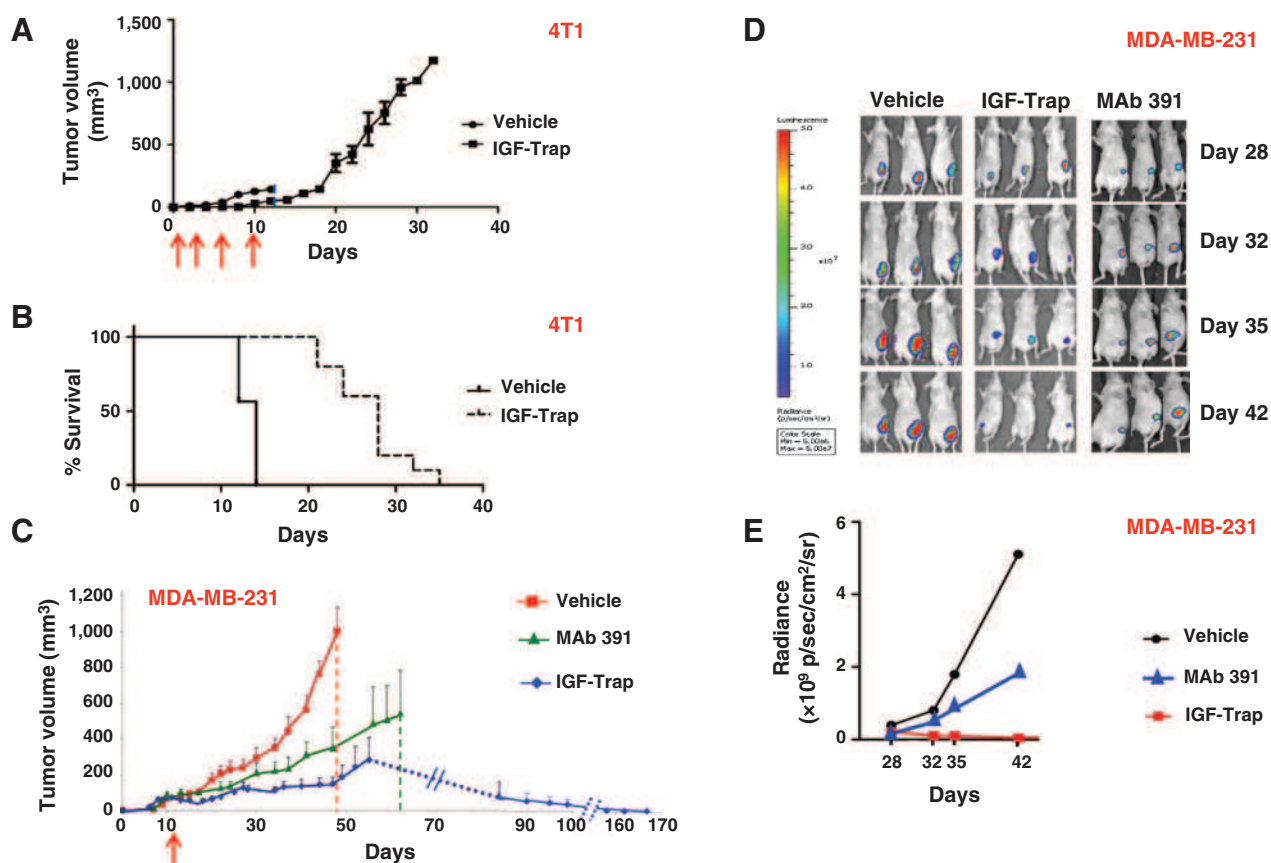
Having established the favorable pharmacokinetic properties of the IGF-Trap, we next assessed its therapeutic efficacy in several metastatic carcinoma models. Therapeutic effects were evaluated in two orthotopic breast carcinoma models, namely, the murine mammary carcinoma 4T1 (28) and triple-negative human breast carcinoma MDA-MB-231 cells (44, 49). Balb/c female mice, orthotopically injected with 10^5 4T1 cells in the MFP, received a total of 4 i.v. injections of the IGF-Trap; 10 mg/kg at 4 and 72 hours and 5 mg/kg at 6 and 10 days after tumor inoculation (Fig. 4A, red arrows). Local MFP tumors grew rapidly in all nontreated mice, and these mice were moribund by day 14 after tumor inoculation (Fig. 4A and B). In treated mice, however, tumors did not significantly progress for the duration of IGF-Trap treatment. Tumor growth was seen only after cessation of treatment (day 14 onward, Fig. 4A) and mice survived for up to 35 days after tumor injection (Fig. 4B; $P < 0.01$ using both the Mantel–Cox and Gehan–Breslow–Wilcoxon tests).

To test the effect of the IGF-Trap on the growth of human breast carcinoma cells, 10^6 MD-MBA-231 cells were implanted with Matrigel in the MFP of nu/nu mice. When tumors were established (50–100 mm³; day 11, Fig. 4C, red arrow), the animals were randomized for i.v. injection with 5 mg/kg of the IGF-Trap or vehicle as control, twice weekly, up to day 33. An additional group of mice was injected with 5 to 10 mg/kg of the anti-IGFIR MAb 391 (K_D 0.02 nmol/L; ref. 29). Mice in the control group were all moribund by day 48 (Fig. 4C, red dashed line). In the IGF-Trap-treated group, tumors did not progress during treatment. Growth arrest followed by complete regression (and long-term survival) was seen in 2 of 5 mice (dotted line). In 3 of 5 mice, tumors began to grow only 20 days after the last treatment was administered (day 53) and morbidity eventually developed in these mice by day 85 following tumor injection (Fig. 4C). In comparison, the effect of MAb 391 on tumor growth was more variable and limited with 2 of 5 mice showing progressive tumor growth at a rate similar to controls and 3 of 5 having reduced tumor growth rate, but no growth arrest, during treatment ($P > 0.05$ from days 10–41). Significantly, no complete regressions were observed in this treatment group, and morbidity was observed from day 65 onward (Fig. 4C, green dashed line). Longitudinal bioluminescence imaging of the tumors showed an increase in signal intensity in the control and MAb 391-treated groups and a marked reduction in signal in the IGF-Trap-treated group over time (Fig. 4D and E).

The IGF-Trap inhibits experimental liver metastasis of colon and lung carcinoma cells

Cancer metastasis to vital organs such as the liver and lung is the major cause of cancer-related death. We assessed the ability of the IGF-Trap to inhibit the growth of metastatic cancer cells in the liver. Mice were injected with colon carcinoma MC-38 or lung carcinoma H-59 cells via the intrasplenic/portal route to generate experimental liver metastases and treated 24 hours later, when micrometastases began to develop (50), with 2 to 10 mg/kg IGF-

Wang et al.

**Figure 4.**

Growth arrest and regression of mammary tumors in mice injected therapeutically with the IGF-Trap. Balb/c mice were injected into the MFP with 5×10^4 4T1 cells (A and B). Intravenous IGF-Trap injections were administered 4 hours and 3, 6, and 10 days (arrows) after tumor inoculation (10 mg/kg for the first 2 injections and 5 mg/kg subsequently). Shown in A are mean tumor volumes (\pm SD) and in B a Kaplan-Meier survival curve ($P < 0.01$ using Mantel-Cox or Gehan-Breslow-Wilcoxon Tests). Nu/nu mice (5–8 per group) were injected in the MFP with 10^6 MDA-MB-231 cells in Matrigel (C–E). Mice were randomized when the tumors measured 50 to 100 mm³ (day 11, arrow) and injected i.v. with 5 mg/kg IGF-Trap, 5 to 10 mg/kg MAb 391, or vehicle, twice weekly up to day 33. Mean tumor volumes (and SD) are shown in C. Red dashed line, the time when all control mice were moribund; green dashed line, when morbidity was seen in the MAb 391-treated group. Mean tumor volumes in the IGF-Trap-treated were significantly lower than controls ($P < 0.05$) from day 20 onwards and in the MAb 391-treated group on days 44 and 48 only. D and E, longitudinal bioluminescence images obtained at the indicated days after tumor injection (D) and bioluminescence signal intensity values in the three groups (E), as a function of time based on 3 to 5 mice per group.

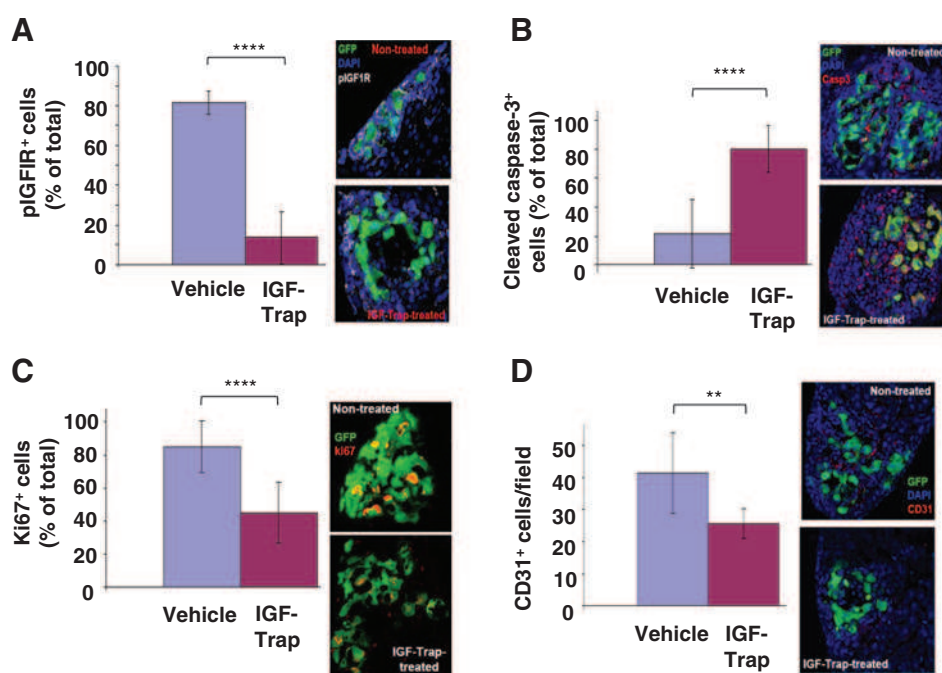
Trap or vehicle, followed by one or two additional injections as indicated. Liver metastases were enumerated and sized 18 days after tumor injection. In a separate experiment, and as a comparison, we also treated MC-38-inoculated mice, twice daily for 5 days with 50 mg/kg rhIGFBP-1 (a 10-fold higher concentration than the IGF-Trap), which was confirmed by SPR to be functionally active (Supplementary Table S2), with binding affinities for hIGFI ($K_D \sim 2$ nmol/L) similar to those of the IGF-Trap ($K_D \sim 5$ nmol/L). The results show that three IGF-Trap injections administered 1, 4, and 8 days after tumor inoculation markedly reduced the number and size of MC-38 liver metastases in a dose-dependent manner (Fig. 5A and B), whereas treatment with IGF-BP-1 had no significant effect on liver metastases formation (Fig. 5C). The number of H-59 metastases was also significantly reduced following two injections of IGF-Trap, 1 and 5 days after tumor inoculation (Fig. 5D and E). Although in some IGF-Trap-treated mice, the numbers of liver metastases were within the range observed in some untreated mice, these metastases were significantly smaller in size, suggesting that some surviving tumor cells

may have resumed growth upon cessation of treatment on days 5 (H-59) or 8 (MC-38) and indicating that prolonged treatment and/or increased doses could probably improve outcome. Taken together, these results indicated that the IGF-Trap could block tumor cell growth even in an IGF-rich microenvironment, such as the liver.

The IGF-Trap blocks IGFIR signaling and functions in tumor cells *in vivo*

The mechanism of action of the IGF-Trap was assessed in mice that received an intrasplenic/portal injection of 10^5 GFP-tagged H-59 cells followed by 5 mg/kg IGF-Trap (or vehicle), 1 and 3 days later. Livers removed on day 6 were analyzed by IHC using an anti-IGFIR antibody. The results (Fig. 6A) showed that as a consequence of this treatment, signaling of the IGFIR was significantly inhibited. In turn, the proportion of tumor cells undergoing apoptosis within the hepatic micrometastases was significantly increased (Fig. 6B), whereas the proportion of proliferating tumor cells significantly decreased (Fig. 6C). Moreover, vessel density in

Wang et al.

**Figure 6.**

The IGF-Trap inhibits IGFIR signaling and functions *in vivo*. Mice were injected by the intrasplenic/portal route with 10^5 GFP-tagged H-59 cells followed by 5 mg/kg IGF-Trap or vehicle, 1 and 3 days later. Livers were obtained on day 6, and 10- μ m cryostat sections were immunostained with pIGFIR (A), cleaved caspase-3 (B), Ki67 (C), and CD31 (D) in the presence of DAPI (1:2,000). For each treatment group, 11 to 16 sections were analyzed, and the percentage of tumor cells (green) that were positive for the indicated marker (A–C) or the number of CD31⁺ endothelial cells per field ($\times 20$ objective) was calculated. Shown are representative, merged confocal images (A–D) and mean (\pm SD) of percentage of immunolabeled tumor (A–C) or endothelial (D) cells per field. **, $P < 0.01$; ****, $P < 0.001$.

domain (18). IGFIR, however, is the only high affinity binding receptor for IGF1, and fusion to a second ligand-binding site was therefore not required for efficient trapping of circulating IGF1 in the treated mice. IGFII can also bind to IGFIR, but this second receptor does not have intracellular signaling functions and acts, in fact, to reduce IGFII bioavailability for IGFIR. Binding of free IGFII to IGFIR does not therefore represent an obstacle to tumor growth inhibition. Finally, IGF1 is the major circulating IGFIR ligand in adult mice, but IGFII is the major plasma IGFIR ligand in man (58). In addition, IGFII can also bind to the insulin receptor IR-A to activate signaling in tumor cells. Our SPR data confirmed that the IGF-Trap can bind IGFII with high affinity, and we have also shown that the IGF-Trap is able to block IGFII-induced migration in two different tumor cell types *in vitro*, suggesting that it is functionally active against IGFII. Although this is suggestive of anti-IGFII potency, the ability of the IGF-Trap to efficiently block the effects of circulating and paracrine or autocrine IGFII *in vivo* in the clinical setting cannot be conclusively determined based on the preclinical mouse models and *in vitro* assays used in this study and it remains to be verified in the clinic. Our finding that higher concentrations of the Trap were required to achieve an inhibition of IGFII-mediated migration that is similar in magnitude to inhibition of IGF1-induced functions is consistent with the reduced affinity of the IGF-Trap for IGFII, as was shown in Fig. 1.

The IGF-Trap could inhibit IGFIR signaling in tumor cells *in vitro* and *in vivo* and, as a result, increased apoptosis and reduced the proliferation of these cells. We also observed a reduction in tumor-associated angiogenesis. The causal relationship between these effects may involve reciprocal mechanisms. IGF ligands can promote angiogenesis by upregulating tumor-derived VEGF production or via direct effects on the endothelial cells (1). Although the observed reduction in angiogenesis may therefore be secondary to increased tumor cell apoptosis, it is also possible that (i) reduced neovascularization may contribute to increased tumor cell death or (ii) both mechanisms contribute to the observed

reduction in tumor growth. It should also be noted that commercially available anti-pIGFIR antibodies generally cross react with pIR, and we found that the tumor cells used in the present study all express IR-A at different ratios to IGFIR (Supplementary Fig. S6). The reduction of >85% in pIGFIR signal observed in IGF-Trap-treated mice bearing MC-38 metastasis and the marked effects of the IGF-Trap in all tumor models tested, regardless of the expression levels of IR-A suggest that IR-A signaling in the treated mice, if it occurred due to the presence of IGFII, was also highly suppressed.

Of note, we did not observe a major sustained reduction in total circulating IGF1 levels in IGF-Trap-treated mice. This suggests that method used for IGF1 quantification may not distinguish between the Trap-bound and -unbound IGF1 and therefore may not provide a measure of the bioavailable ligand. The IGF-Trap may also act locally, inhibiting paracrine IGF1 activity at the tumor site (59). Our observation that total circulating IGF1 levels did not significantly increase after IGF-Trap injection (although minor increases were observed) may suggest that any increase in IGF1 production that has occurred due to a compensatory feedback loop caused by reduced IGF1 bioavailability (59) may have been offset by coinciding clearance of IGF1:IGF-Trap complexes, thereby masking actual changes to total IGF1 levels. Such changes and also the short duration of the experiments may explain the apparent lack of measurable increase in insulin levels in these mice. In IGF-Trap-injected mice, we observed a gradual decrease in IGF1:Trap complexes following injection. Although the mechanism of Trap clearance remains to be elucidated, proteolytic degradation of circulating complexes has been documented (48) and likely plays a role.

In IGF-Trap preparations, we observed protein species that migrated at a >400 kDa range [high molecular weight (HMW) species] that could be minimized by step elution following Protein A column purification. The appearance of HMW species of Fc fusion proteins was observed by others and attributed to the formation of disulfide bonds between individual Fc

domains (36). These fractions could be minimized when the protein was eluted at pH 4.5 and enriched by elution at pH 3.5. Fractions enriched for HMW proteins had a markedly reduced ligand affinity and a half-life of only 10 hours (data not shown), indicating that they were more rapidly cleared from the circulation and did not contribute significantly to the biologic effects of the Trap.

In mice injected with mammary carcinoma 4T1 cells, we observed that tumors did not grow during the course of IGF-Trap treatment, but growth resumed several days after cessation of treatment. Notably, we observed that whereas all the mice in the untreated group were moribund with metastatic disease by day 14 after tumor injection (when the mean tumor volume in that group was $< 200 \text{ mm}^3$), mice in the treatment group survived for up to 35 days with significantly larger tumors (mean tumor volumes exceeding 1 cm^3). Although the underlying factors remain to be fully elucidated, the data suggest that IGF-Trap treatment resulted in the elimination of a more aggressive tumor subpopulation, consequently shifting the tumor phenotype. This implies that different subpopulations within the tumor may have different susceptibilities to reduced IGFI bioavailability with highly aggressive subpopulations being particularly sensitive to the treatment.

The IGF-Trap could have several advantages over IGF-targeting drugs currently in clinical use. Because of its high specificity for IGF ligands and low affinity for insulin, deleterious effects on IR signaling should be minimized with the IGF-Trap. Indeed, we previously reported that the sustained production of an IGFI receptor decoy in mice did not significantly affect glucose homeostasis (24) and, similarly, observed here that insulin levels in IGF-Trap-treated mice were unaltered relative to controls. Moreover, the IGF-Trap binds IGFI with high affinity and could suppress IGFI functions *in vitro*, suggesting that unlike IGFI-targeting antibodies (14), the IGF-Trap could potentially block compensatory IGFI/IR-A signaling, when administered as a drug in the clinical setting. The possibility that insulin/IR signaling may still provide a resistance mechanism for tumor cells expressing both receptors cannot, however, be ruled out.

The therapeutic benefits of the IGF-Trap in comparison with other agents, such as antibodies, that bind both IGFI and IGFI, (e.g., MEDI-573 and BI 8368456) can ultimately be determined only in a clinical setting. However, we have shown here that the IGF-Trap could inhibit several tumor cell properties essential for metastasis, such as migration and invasion, and also found that it blocked the growth and metastasis of several aggressive tumor types *in vivo*. These unique properties (not documented for the antibodies) could potentially prove to be an asset in clinical management of aggressive malignancies. It also remains to be seen whether some of the adverse effects reported for MEDI-

573 (e.g., anemia and leucopenia; ref. 60) could be averted by the use of a Trap.

In the present study, significant reductions in tumor growth were observed using the IGF-Trap as a "stand-alone" single agent. In the liver metastasis models, we have observed either a modest or a lack of therapeutic effect in some cases, possibly as a result of the relatively short duration of the treatment. Moreover, liver metastasis is a complex multifactorial process (61), and a more limited therapeutic effect of the IGF-Trap on some metastases may suggest that the IGF axis may not be the predominant driver of metastatic growth in some tumor cells or that compensatory mechanisms can bypass the dependency on IGF for growth. Combination therapies in which several growth and survival factors are targeted may ultimately be required to achieve the desired therapeutic effects in metastatic disease.

Disclosure of Potential Conflicts of Interest

No potential conflicts of interest were disclosed.

Authors' Contributions

Conception and design: S.M. Elahi, B. Massie, P. Brodt

Development of methodology: N. Wang, S.M. Elahi, M.A. Hancock, G.E. Rowe, H. Aomari, Y. Durocher, P. Brodt

Acquisition of data (provided animals, acquired and managed patients, provided facilities, etc.): N. Wang, R.F. Rayes, S.M. Elahi, M.A. Hancock, S. Tabariès, P.M. Siegel, P. Brodt

Analysis and interpretation of data (e.g., statistical analysis, biostatistics, computational analysis): N. Wang, R.F. Rayes, S.M. Elahi, Y. Lu, M.A. Hancock, B. Massie, S. Hossain, M. Pinard, P. Brodt

Writing, review, and/or revision of the manuscript: R.F. Rayes, S.M. Elahi, M.A. Hancock, B. Massie, S. Hossain, P.M. Siegel, P. Brodt

Administrative, technical, or material support (i.e., reporting or organizing data, constructing databases): N. Wang, S.M. Elahi, M. Pinard, P. Brodt

Study supervision: Y. Durocher, P. Brodt

Other (development of purification methodology): G.E. Rowe

Acknowledgments

The McGill SPR-MS Facility thanks the Canada Foundation for Innovation (CFI) and Canadian Institutes for Health Research (CIHR) for infrastructure support.

Grant Support

This work was supported mainly by a grant from the Quebec Ministry of Economic Development and by a grant from the Terry Fox Research Institute (to P. Brodt and B. Massie). R.F. Rayes was supported by the Henry R. Shibata Fellowship from the Cedars Cancer Institute and by a Mathematics of Information Technology and Complex Systems (MITACS) internship.

The costs of publication of this article were defrayed in part by the payment of page charges. This article must therefore be hereby marked *advertisement* in accordance with 18 U.S.C. Section 1734 solely to indicate this fact.

Received September 3, 2014; revised January 13, 2015; accepted February 1, 2015; published OnlineFirst February 11, 2015.

References

- Samani AA, Yakar S, LeRoith D, Brodt P. The role of the IGF system in cancer growth and metastasis: overview and recent insights. *Endocr Rev* 2007;28:20–47.
- Zhang D, Samani AA, Brodt P. The role of the IGF-I receptor in the regulation of matrix metalloproteinases, tumor invasion and metastasis. *Horm Metab Res* 2003;35:802–8.
- Seccareccia E, Brodt P. The role of the insulin-like growth factor-I receptor in malignancy: an update. *Growth Horm IGF Res* 2012;22:193–9.
- Sachdev D. Drug evaluation: CP-751871, a human antibody against type I insulin-like growth factor receptor for the potential treatment of cancer. *Curr Opin Mol Ther* 2007;9:299–304.
- Sachdev D, Singh R, Fujita-Yamaguchi Y, Yee D. Down-regulation of insulin receptor by antibodies against the type I insulin-like growth factor receptor: implications for anti-insulin-like growth factor therapy in breast cancer. *Cancer Res* 2006;66:2391–402.
- Gao J, Chesebrough JW, Cartledge SA, Ricketts SA, Incognito L, Veldman-Jones M, et al. Dual IGF-I/II-neutralizing antibody MEDI-573 potently inhibits IGF signaling and tumor growth. *Cancer Res* 2011;71:1029–40.
- Friedbichler K, Hofmann MH, Kroez M, Ostermann E, Lamche HR, Koessl C, et al. Pharmacodynamic and antineoplastic activity of BI 836845, a fully human IGF ligand-neutralizing antibody, and mechanistic rationale for combination with rapamycin. *Mol Cancer Ther* 2014;13:399–409.

8. Alami N, Page V, Yu Q, Jerome L, Paterson J, Shiry L, et al. Recombinant human insulin-like growth factor-binding protein 3 inhibits tumor growth and targets the Akt pathway in lung and colon cancer models. *Growth Horm IGF Res* 2008;18:487–96.
9. Van den Berg CL, Cox GN, Stroh CA, Hilsenbeck SG, Weng CN, McDermott MJ, et al. Polyethylene glycol conjugated insulin-like growth factor binding protein-1 (IGFBP-1) inhibits growth of breast cancer in athymic mice. *Eur J Cancer* 1997;33:1108–13.
10. Arnaldez FI, Helman LJ. Targeting the insulin growth factor receptor 1. *Hematol Oncol Clin North Am* 2012;26:527–42, vii–viii.
11. Chen HX, Sharon E. IGF-1R as an anti-cancer target—trials and tribulations. *Chinese J Cancer* 2013;32:242–52.
12. Pollak M. The insulin and insulin-like growth factor receptor family in neoplasia: an update. *Nat Rev Cancer* 2012;12:159–69.
13. Gualberto A, Pollak M. Emerging role of insulin-like growth factor receptor inhibitors in oncology: early clinical trial results and future directions. *Oncogene* 2009;28:3009–21.
14. Avnet S, Sciacca L, Salerno M, Gancitano G, Cassarino MF, Longhi A, et al. Insulin receptor isoform A and insulin-like growth factor II as additional treatment targets in human osteosarcoma. *Cancer Res* 2009;69:2443–52.
15. Buck E, Gokhale PC, Koujak S, Brown E, Eyzaguirre A, Tao N, et al. Compensatory insulin receptor (IR) activation on inhibition of insulin-like growth factor-1 receptor (IGF-1R): rationale for cotargeting IGF-1R and IR in cancer. *Mol Cancer Ther* 2010;9:2652–64.
16. Frasca F, Pandini G, Scalia P, Sciacca L, Mineo R, Costantino A, et al. Insulin receptor isoform A, a newly recognized, high-affinity insulin-like growth factor II receptor in fetal and cancer cells. *Mol Cell Biol* 1999;19:3278–88.
17. Girmita L, Worrall C, Takahashi S, Seregard S, Girmita A. Something old, something new and something borrowed: emerging paradigm of insulin-like growth factor type 1 receptor (IGF-1R) signaling regulation. *Cell Mol Life Sci* 2014;71:2403–27.
18. Holash J, Davis S, Papadopoulos N, Croll SD, Ho L, Russell M, et al. VEGF-Trap: a VEGF blocker with potent antitumor effects. *Proc Natl Acad Sci U S A* 2002;99:11393–8.
19. Trieu Y, Wen XY, Skinnider BF, Bray MR, Li Z, Claudio JO, et al. Soluble interleukin-13Ralpha2 decoy receptor inhibits Hodgkin's lymphoma growth in vitro and in vivo. *Cancer Res* 2004;64:3271–5.
20. Tseng JF, Farnedo FA, Kisker O, Becker CM, Kuo CJ, Folkman J, et al. Adenovirus-mediated delivery of a soluble form of the VEGF receptor Flk1 delays the growth of murine and human pancreatic adenocarcinoma in mice. *Surgery* 2002;132:857–65.
21. Messori A, Santarlasci B, Vaiani M. New drugs for rheumatoid arthritis. *N Engl J Med* 2004;351:937–8.
22. D'Ambrosio C, Ferber A, Resnicoff M, Baserga R. A soluble insulin-like growth factor I receptor that induces apoptosis of tumor cells in vivo and inhibits tumorigenesis. *Cancer Res* 1996;56:4013–20.
23. Samani AA, Chevet E, Fallavollita L, Galipeau J, Brodt P. Loss of tumorigenicity and metastatic potential in carcinoma cells expressing the extracellular domain of the type 1 insulin-like growth factor receptor. *Cancer Res* 2004;64:3380–5.
24. Wang N, Fallavollita L, Nguyen L, Burnier J, Rafei M, Galipeau J, et al. Autologous bone marrow stromal cells genetically engineered to secrete an igf-I receptor decoy prevent the growth of liver metastases. *Mol Ther* 2009;17:1241–9.
25. Wang N, Lu Y, Pinard M, Pilotte A, Gilbert R, Massie B, et al. Sustained production of a soluble IGF-I receptor by gutless adenovirus-transduced host cells protects from tumor growth in the liver. *Cancer Gene Ther* 2013;20:229–36.
26. Didion JP, Buus RJ, Naghashfar Z, Threadgill DW, Morse HC3rd, de Villena FP. SNP array profiling of mouse cell lines identifies their strains of origin and reveals cross-contamination and widespread aneuploidy. *BMC Genomics* 2014;15:847.
27. Brodt P. Characterization of two highly metastatic variants of Lewis lung carcinoma with different organ specificities. *Cancer Res* 1986;46:2442–8.
28. Tabaries S, Dong Z, Annis MG, Omeroglu A, Pepin F, Ouellet V, et al. Claudin-2 is selectively enriched in and promotes the formation of breast cancer liver metastases through engagement of integrin complexes. *Oncogene* 2011;30:1318–28.
29. Calzone FJ, Cajulis E, Chung YA, Tsai MM, Mitchell P, Lu J, et al. Epitope-specific mechanisms of IGF1R inhibition by ganitumab. *PLoS ONE* 2013;8:e55135.
30. Gilbert RBS, Massie B. Protein production using lentiviral vectors. In: Dyson MRDY, editor. *Methods express: expression systems*. Oxfordshire: Scion Publishing Ltd; 2007. p. 241–58.
31. Gaillet B, Gilbert R, Broussau S, Pilotte A, Malenfant F, Mullick A, et al. High-level recombinant protein production in CHO cells using lentiviral vectors and the cumate gene-switch. *Biotechnol Bioeng* 2010;106:203–15.
32. Myszkka DG. Improving biosensor analysis. *J Mol Recognit* 1999;12:279–84.
33. Beattie J, Phillips K, Shand JH, Szymanowska M, Flint DJ, Allan GJ. Molecular interactions in the insulin-like growth factor (IGF) axis: a surface plasmon resonance (SPR) based biosensor study. *Mol Cell Biochem* 2008;307:221–36.
34. Forbes BE, Hartfield PJ, McNeil KA, Surinya KH, Milner SJ, Cosgrove LJ, et al. Characteristics of binding of insulin-like growth factor (IGF)-I and IGF-II analogues to the type 1 IGF receptor determined by BIAcore analysis. *Eur J Biochem* 2002;269:961–8.
35. Jansson M, Dixelius J, Uhlen M, Nilsson BO. Binding affinities of insulin-like growth factor-I (IGF-I) fusion proteins to IGF binding protein 1 and IGF-I receptor are not correlated with mitogenic activity. *FEBS Lett* 1997;416:259–64.
36. Surinya KH, Forbes BE, Occhiodoro F, Booker GW, Francis GL, Siddle K, et al. An investigation of the ligand binding properties and negative cooperativity of soluble insulin-like growth factor receptors. *J Biol Chem* 2008;283:5355–63.
37. Brodt P, Fallavollita L, Khatib AM, Samani AA, Zhang D. Cooperative regulation of the invasive and metastatic phenotypes by different domains of the type I insulin-like growth factor receptor beta subunit. *J Biol Chem* 2001;276:33608–15.
38. Burnier JV, Wang N, Michel RP, Hassanain M, Li S, Lu Y, et al. Type IV collagen-initiated signals provide survival and growth cues required for liver metastasis. *Oncogene* 2011;30:3766–83.
39. Rahim S, Uren A. A real-time electrical impedance based technique to measure invasion of endothelial cell monolayer by cancer cells. *J Vis Exp* 2011;pii:2792.
40. Auguste A, Fallavollita L, Wang N, Bikfalvi A, Brodt P. The host inflammatory response promotes liver metastasis by increasing tumor cell arrest and extravasation. *Am J Pathol* 2007;170:1781–92.
41. Long L, Rubin R, Baserga R, Brodt P. Loss of the metastatic phenotype in murine carcinoma cells expressing an antisense RNA to the insulin-like growth factor receptor. *Cancer Res* 1995;55:1006–9.
42. Long L, Rubin R, Brodt P. Enhanced invasion and liver colonization by lung carcinoma cells overexpressing the type 1 insulin-like growth factor receptor. *Exp Cell Res* 1998;238:116–21.
43. Jansson M, Hallen D, Koho H, Andersson G, Berghard L, Heidrich J, et al. Characterization of ligand binding of a soluble human insulin-like growth factor I receptor variant suggests a ligand-induced conformational change. *J Biol Chem* 1997;272:8189–97.
44. Davison Z, de Blacquièrè GE, Westley BR, May FE. Insulin-like growth factor-dependent proliferation and survival of triple-negative breast cancer cells: implications for therapy. *Neoplasia* 2011;13:504–15.
45. Zhang D, Brodt P. Type 1 insulin-like growth factor regulates MT1-MMP synthesis and tumor invasion via PI 3-kinase/Akt signaling. *Oncogene* 2003;22:974–82.
46. Datta SR, Dudek H, Tao X, Masters S, Fu H, Gotoh Y, et al. Akt phosphorylation of BAD couples survival signals to the cell-intrinsic death machinery. *Cell* 1997;91:231–41.
47. Lin YS, Nguyen C, Mendoza JL, Escandon E, Fei D, Meng YG, et al. Preclinical pharmacokinetics, interspecies scaling, and tissue distribution of a humanized monoclonal antibody against vascular endothelial growth factor. *J Pharmacol Exp Ther* 1999;288:371–8.
48. Rudge JS, Holash J, Hylton D, Russell M, Jiang S, Leidich R, et al. VEGF Trap complex formation measures production rates of VEGF, providing a biomarker for predicting efficacious angiogenic blockade. *Proc Natl Acad Sci U S A* 2007;104:18363–70.
49. Mourskaia AA, Dong Z, Ng S, Banville M, Zwaagstra JC, O'Connor-McCourt MD, et al. Transforming growth factor-beta1 is the predominant isoform required for breast cancer cell outgrowth in bone. *Oncogene* 2009;28:1005–15.

50. Auguste P, Fallavollita L, Wang N, Burnier J, Bikfalvi A, Brodt P. The host inflammatory response promotes liver metastasis by increasing tumor cell arrest and extravasation. *Am J Pathol* 2007;170:1781–92.
51. Rechler MM. Insulin-like growth factor binding proteins. *Vitam Horm* 1993;47:1–114.
52. Korhonen R, Moilanen E. Abatacept, a novel CD80/86-CD28 T cell co-stimulation modulator, in the treatment of rheumatoid arthritis. *Basic Clin Pharmacol Toxicol* 2009;104:276–84.
53. Mohler KM, Torrance DS, Smith CA, Goodwin RC, Stremel KE, Fung VP, et al. Soluble tumor necrosis factor (TNF) receptors are effective therapeutic agents in lethal endotoxemia and function simultaneously as both TNF carriers and TNF antagonists. *J Immunol* 1993;151:1548–61.
54. Poppel K, Crawford D, Beutler B. A tumor necrosis factor (TNF) receptor-IgG heavy chain chimeric protein as a bivalent antagonist of TNF activity. *J Exp Med* 1991;174:1483–9.
55. Chu QS. Aflibercept (AVE0005): an alternative strategy for inhibiting tumour angiogenesis by vascular endothelial growth factors. *Expert Opin Biol Ther* 2009;9:263–71.
56. Harding TC, Long L, Palencia S, Zhang H, Sadra A, Hestir K, et al. Blockade of nonhormonal fibroblast growth factors by FP-1039 inhibits growth of multiple types of cancer. *Sci Transl Med* 2013; 5:178ra39.
57. Huang C. Receptor-Fc fusion therapeutics, traps, and MIMETIBODY technology. *Curr Opin Biotechnol* 2009;20:692–9.
58. LeRoith D, Roberts CT, Jr. Insulin-like growth factors and their receptors in normal physiology and pathological states. *J Pediatr Endocrinol* 1993; 6:251–5.
59. Le Roith D, Bondy C, Yakar S, Liu JL, Butler A. The somatomedin hypothesis: 2001. *Endocr Rev* 2001;22:53–74.
60. Gao J, Chang YS, Jallal B, Viner J. Targeting the insulin-like growth factor axis for the development of novel therapeutics in oncology. *Cancer Res* 2012;72:3–12.
61. Van den Eynden GG, Majeed AW, Illemann M, Vermeulen PB, Bird NC, Hoyer-Hansen G, et al. The multifaceted role of the microenvironment in liver metastasis: biology and clinical implications. *Cancer Res* 2013; 73:2031–43.

Molecular Cancer Therapeutics

The IGF-Trap: Novel Inhibitor of Carcinoma Growth and Metastasis

Ni Wang, Roni F. Rayes, Seyyed Mehdy Elahi, et al.

Mol Cancer Ther 2015;14:982-993. Published OnlineFirst February 11, 2015.

| | |
|-------------------------------|---|
| Updated version | Access the most recent version of this article at: doi: 10.1158/1535-7163.MCT-14-0751 |
| Supplementary Material | Access the most recent supplemental material at: http://mct.aacrjournals.org/content/suppl/2015/02/11/1535-7163.MCT-14-0751.DC1.html |

| | |
|-----------------------|--|
| Cited articles | This article cites 60 articles, 22 of which you can access for free at: http://mct.aacrjournals.org/content/14/4/982.full.html#ref-list-1 |
|-----------------------|--|

| | |
|-----------------------------------|---|
| E-mail alerts | Sign up to receive free email-alerts related to this article or journal. |
| Reprints and Subscriptions | To order reprints of this article or to subscribe to the journal, contact the AACR Publications Department at pubs@aacr.org . |
| Permissions | To request permission to re-use all or part of this article, contact the AACR Publications Department at permissions@aacr.org . |